July 23-27, 2006, Vancoucer, BC, Canada

PVP2006-ICPVT-11-93548

SPECTRA THERMAL FATIGUE TESTS UNDER FREQUENCY CONTROLLED FLUID TEMPERATURE VARIATION - TRANSIENT TEMPERATURE MEASUREMENT TESTS -

Nobuchika KAWASAKI, Sumio KOBAYASHI, Shinichi HASEBE, and Naoto KASAHARA
/Japan Atomic Energy Agency, 4002 Narita, Oarai, Ibaraki, 311-13, Japan

ABSTRACT

The coolant leakage by thermal striping phenomenon should be prevented at nuclear power plants and a lot of efforts are made to develop its evaluation methods. The frequency transfer function method can be used to obtain temperature and stress response to fluid temperature history using transfer function models; therefore it is considered as an excellent evaluation method.

To measure temperature response of structures to fluid temperature variations and to confirm their frequency characteristics, transient temperature measurement tests were performed by JAEA. In the transient temperature measurement tests, three different frequencies of sinusoidal fluid temperature waves (0.05, 0.2, 0.5Hz) were controlled using frequency controlled thermal fatigue test equipment (SPECTRA) and temperature responses at inner and outer piping surfaces were measured along the test sections.

Frequency effects on temperature attenuation during transfer process from fluid to structures were confirmed and the effective heat transfer function in frequency transfer function method was verified by transient temperature measurement test results.

NOMENCLATURE

T_f, $T_f^* = T_f / T_0$: Fluid temperature
T_0 : Source fluid temperature difference
T_s, $T_s^* = T_s / T_0$: Structural temperature
$Bi = hL / \lambda$: Biot number
$Nu = hD / \lambda$: Nusselt number
Pe : Peclet number
σ, $\sigma^* = \sigma / \{ E\alpha T_0 / (1-\nu) \}$: Stress
h : Heat transfer coefficient
L : Wall thickness of structure
D : Inner diameter of test piece
λ : Heat conductivity
E : Young's modulus of structural material
x, $x^* = x/L$: Depth into wall direction
α : Linear expansion coefficient of material
ν : Poisson's ratio
$H(Bi, j\omega)$: Effective heat transfer function
$S(x^*, Bi, j\omega, Rm, Rb)$: Effective thermal stress function
R_m, R_b : Constraint efficiency factors[6],[9] $0 \le R \le 1$, Constraint free=0, Perfect constraint=1
$\Im$: Fourier transform
j : Imaginary number
ω, $\omega^* = L\sqrt{\omega / 2\kappa}$: Angular velocity
κ : Thermal diffusivity of structural material
t : Time
Suffix * : Non-dimensional number

INTRODUCTION

At an incomplete mixing area of high and low temperature fluids in nuclear components, fluid temperature fluctuates with random frequencies. It induces random variations of local temperature gradients in structural walls of pipes, which lead to cyclic thermal stresses (Fig.1). When thermal stresses and number of cycles are large, there are possibilities of crack initiations and propagations. This coupled thermal hydraulic and thermal mechanical phenomenon is called thermal striping, which should be prevented.

Temperature responses of structures to fluid have characteristics described in Fig.2. There are attenuations of temperature fluctuation ranges in the heat transfer process. When frequencies of fluid fluctuation become higher, attenuation is larger by delay of structural response, and temperature fluctuation range in structure $\Delta T_s(x)$ is smaller in spite of the same magnitude of a fluid temperature fluctuation.
In this paper, frequency effects on temperature attenuation during transfer process from fluid temperature fluctuations to surfaces is confirmed and the evaluation method based on frequency transfer functions is verified by transient temperature measurement tests using SPECTRA

TEST FACILITY AND TEST PIECE

SPECTRA test facility has a hot sodium line with an electric heater and a cold one with an air-cooler. Electromagnetic pumps installed in each line drive these 600°C and 250°C sodium and mix them in the mixing tee. SPECTRA is able to control precisely sodium temperature variation under various frequencies with constant flow rate in the test section as shown in Fig.3. Specifications of SPECTRA are explained in Table1, and in these tests, three sinusoidal waves with different frequencies are selected to confirm frequency effect.

Fig. 4 illustrates the test section of SPECTRA. Thin tubular upstream part and thick tubular downstream test piece compose the test section. The test section is fabricated by 304 stainless steel. The inner diameter of test section is 66.9mm and the thicknesses of thin part and thick test piece are 4.7 and 11.1mm respectively. The lengths of upstream thin part and downstream test piece are about 5D and 25D respectively. Thermo-couples are installed along the axis of test section. To measure time histories of fluid temperature fluctuations in main flows, several thermo-couples are installed at 3mm inside from the inner surfaces of test pieces. To measure surface temperature histories, several thermo-couples are installed on the inner and the outer surfaces of test pieces. These thermo-couples are type K (chromel / alumel) ones, where sheath diameter is 1.0mm and thickness of thermo-couple's tip is finished to 0.2mm.

In these tests, the axial positions of upstream thermo-couples in fluid are 10, 60, 120, 180, 260mm from the end of mixing tee and these of upstream thermo-couples at structure surface are 30, 90, 150, 230mm. In the downstream test piece, thermo-couples are installed at 372.4mm (TS-1A) and 1772.4mm (TS-8A) for both fluid and inner surface. At all positions, thermo-couples are installed at upside and downside of the pipe as in Fig. 4.

MEASURED TEMPERATURE AND ITS FREQUENCY CHARACTERISTICS

Fig. 5, 6, and 7 are the measured temperature histories of fluid and inner surfaces under three different frequency conditions. Fluid temperature ranges are controlled as 200°C (about 325°C to 525°C) at TS-1A for all frequency conditions and their frequencies are 0.05, 0.2, 0.5Hz. In the previous figures, fluid and inner surface temperatures at TS-1A and TS-8A are plotted as representative temperature histories.

Fluid temperature fluctuations are smoothly controlled as sinusoidal waves and inner surface temperatures respond as delayed and attenuated sinusoidal waves. When the frequency of fluid fluctuation becomes higher, the inner surface temperature fluctuation range becomes smaller in spite of the same magnitude of the fluid temperature fluctuation range at TS-1A. The fluid temperature fluctuation ranges at TS-8A are different among three frequency conditions; however the attenuation from fluid to structural surface becomes larger when the frequency of fluid fluctuation is higher.

The axial distributions of temperature ranges for each frequency conditions are in Fig. 8, 9, and 10. In the figures the temperature ranges of fluid, inner surfaces, and outer surfaces are plotted along the test sections. In the downstream test pieces, the attenuation from fluid to structural surface becomes larger when the frequency of fluid fluctuation is higher. About the attenuation from structural inner surface to outer surface, the same frequency effect can be observed. For the upstream thin part these frequency effects can be observed all along the tube from fluid to inner surface and from inner surface to outer surface.

HEAT TRANSFER COEFFICIENTS

Heat transfer coefficients for each frequency condition are calculated using measured temperature ranges and average heat conductivity λ(425°C)=21.16[W/mK] by Biot number decided from equation (3). Fig.11, 12, and 13 are calculated heat transfer coefficients along axial directions.

In the upstream thin parts which are transition regions of turbulent flow, calculated heat transfer coefficients are unstable in axial directions and larger than these in the downstream test pieces. In the downstream test pieces, heat transfer coefficients are constant and steady values and nearly equal to these calculated with Martinelli-Lyon's equation (1) from Ref.[1]. The error ranges between measured heat transfer coefficients from test data and these calculated with Martinelli-Lyon's are within 10% for all frequency conditions. Martinelli-Lyon's equation is a heat transfer equation for fully developed turbulent flow of single-phase liquid metal under uniform heat flux condition. It is said that this equation shows good accordance with experimental data under low impurity condition such as density of oxygen is less than 30ppm from Ref.[2].

Martinelli-Lyon's equation: $$Nu = 7+0.025Pe^{0.8} \quad (1)$$

From this result, there is a possibility to apply heat transfer equations for stationary turbulent flow to unstationary heat flux field like thermal striping phenomena. This consideration is supported by the past similar experiments, hot and cold sodium alternative injection experiment: FAENA [3][4] and triple parallel jets sodium experiment[5]. The experimental results of FAENA show smaller heat transfer coefficients than these with an equation for steady state. The triple parallel jets sodium experiment shows nearly same heat transfer coefficients as these with an equation for steady state.

FREQUENCY TRANSFER FUNCTION METHOD

Frequency transfer function method [6][7][8] can evaluate temperature and stress response to fluid temperature fluctuation using transfer function models. These transfer functions were modeled as functions of temperature frequency and the proposed evaluation procedure is shown as in Fig.14. A fluid temperature fluctuation $T_f^*(j\omega)$ is transferred into a surface temperature fluctuation $T_s^*(0, Bi, j\omega)$ by an effective heat transfer function $H(Bi, j\omega)$. A surface temperature fluctuation $T_s^*(0, Bi, j\omega)$ is transferred into thermal stress $\sigma(x^*, Bi, j\omega, Rm, Rb)$ by an effective thermal stress function $S(x^*, Bi, j\omega, Rm, Rb)$. These transfers are described as follows.

Input of a function is non-dimensional fluid temperature on frequency domain:

$$T_f^*(j\omega) = T_f(j\omega)/T_0 = \Im[T_f(t)/T_0] \tag{2}$$

$$T_s^*(0, Bi, j\omega) = H(Bi, j\omega) T_f^*(j\omega) \tag{3}$$

$$\sigma^*(x^*, Bi, j\omega, R_m, R_b) = H(Bi, j\omega)\, S(x^*, j\omega, R_m, R_b) T_f^*(j\omega) \tag{4}$$

By inverse Fourier transfer and dimensional factors, we can get time histories of thermal stress.

$$\sigma(x, h, t, R_m, R_b) = \frac{E\alpha T_0}{1-\nu}\, \Im^{-1}[\sigma^*(x^*, Bi, j\omega, R_m, R_b)] \tag{5}$$

These transfer functions were theoretically obtained and formulated into design charts as Fig. 15 and 16 [6][7][8][9].

COMPARISON BETWEEN TEST DATA AND EFFECTIVE HEAT TRANSFER FUNCTION

By temperature interpolations of axial directions in Fig. 8, 9, and 10 measured temperature attenuations at each thermo-couple positions are obtained. Non-dimensional angular velocities for 0.05, 0.2, and 0.5 Hz are 0.9, 1.7, 2.8 for upstream thin part respectively, and these are 2.1, 4.1, 6.5 for downstream thick test pieces respectively. The symbols in Fig.17 correspond to measured temperature attenuations. Biot numbers are different in axial direction; therefore the symbols are categorized by Biot number.

In Fig.17, frequency effect on heat transfers were comfirmed by experimental results, where temperature attenuations under higher frequency conditions. With this data the characteristics of effective heat transfer functions in Fig.15 were confirmed qualitatively.

The gains of effective heat transfer functions are calculated with Martinelli-Lyon’s equation for downstream test pieces which are usual plant design regions. The gains of effective heat transfer functions are calculated with Biot number for upstream thin parts. The curves corresponded to calculated gains by effective heat transfer functions are also indicated in Fig.17 for downstream and upstream thin part conditions. For the upstream condition, plural curves whose Biot numbers are 3, 4, 5, and 6 are drawn to cover whole test piece conditions. These calculated curves show quite similar trend against measured temperature attenuations and quite good accordance from quantitative view at each thermo-couple positions.

Fig.18 shows the relationship of temperature ranges at inner surfaces of test pieces between these ranges measured in test and these ranges calculated by gains of effective heat transfer functions. Solid square symbols indicate these for downstream test pieces and open round symbols indicate these for upstream thin parts.

Plotted open round symbols indicate that the effective heat transfer function can predict nearly exact temperature ranges at inner surfaces when Biot number is known. Plotted solid square symbols indicate that the effective heat transfer function can predict temperature ranges at inner surfaces within 5% error range even when Biot number is unknown and the heat transfer equation for stationary turbulent flow is applied.

CONCLUSIONS

Frequency effects on temperature attenuation during transfer process from fluid temperature fluctuations to surfaces were clarified and the effective heat transfer function method was verified by transient temperature measurement tests using frequency controlled thermal fatigue test equipment (SPECTRA) as follows.

1) The measured attenuation from fluid temperature range to structural surface one $(\Delta T_f - \Delta T_s)/\Delta T_f$ become larger when the frequency of fluid fluctuation is higher all along the test sections.

2) Calculated gains by the effective heat transfer function show quite good accordance with measured temperature attenuations. The error ranges between calculated and measured temperature ranges were within 5% even when Biot number is unknown.

Transient temperature measurement tests also show following additional considerations.

In the downstream test pieces where are enough far from mixing tee, heat transfer coefficients are constant and nearly equal to these calculated with Martinelli-Lyon’s equation. There is a possibility to apply heat transfer equations for stationary turbulent flow to unstationary heat flux field like thermal striping phenomena.

ACKNOWLEDGMENTS

The authors wish to thank the following thermal hydraulic specialists: Mr. Oshima, Mr. Kamide, Mr. Kimura (JAEA, Japan) for their advices in fluid dynamics field.

REFERENCES

[1] Lyon, R.N., Liquid metals handbook, Na-NaK supplement, U.S.A.E.C, (1955)

[2] Кириллов, П. Л., Субботин, В. И., Суворов, М. Я., и Троянов, М. Ф., Атомная Энергия, 6, pp382, (1959)

[3] Naoto Kasahara and Yves Lejeail, Thermal fatigue evaluation of cylinders and plates subjected to fluid temperature fluctuation, EMAS, Proc. of Fatigue2002, (2002)

[4] Yves Lejeail and Naoto Kasahara, Thermal fatigue evaluation of cylinders and plates subjected to fluid temperature fluctuations ,Int. J. of fatigue, 27, pp768-772(2005)

[5] Nobuyuki Kimura, Hiroyuki Miyakoshi, Minoru Igarashi, and Hideki Kamide, Study on High Cycle Thermal Fatigue of FBR plants (3) Comparison of Temperature Fluctuation Characteristics between Water and Sodium, JSME annual meeting, vol.2003, No.3,pp209-210,(2003) (in Japanese)

[6] Naoto Kasahara, Hideki Takasho, and Apisara Yacumpai, Structural response function approach for evaluation of thermal striping phenomena, Nuc. Eng. Des., 212, pp281/292, (2002)

[7] Naoto Kasahara and Hideki Takasho, Stress response functions to multi-dimensional spatial fluctuations of fluid temperature, ASME, PVP-Vol.443-1, pp25/31, (2002)

[8] Naoto Kasahara, Masanori Ando, Ichiro Furuhashi, Chen Fuquan, and Hideki Takasho, Frequency transfer function from fluid temperature fluctuations to stress intensity factors, ASME, PVP-Vol.461, pp119/127, (2003)

[9] Nobuchika Kawasaki, Thermal fatigue evaluation of a partially cooled pipe-crack initiation and propagation analysis, 9th German-Japanese seminar Stuttgart, pp5.1/5.20,(2004)

Table 1 Specifications of SPECTRA facility

Sodium temperature	Hot loop 600°C, Cold loop 250°C
Sodium capacity	$11m^3$
Pump	Electric magnetic
Temperature profile	Sinusoidal, Their multiplication
Temperature rage	Up to about 200°C
Frequency	0.025-0.5Hz (2-40sec)
Flow rate	About 300 l/min
Oxygen density	6 ppm

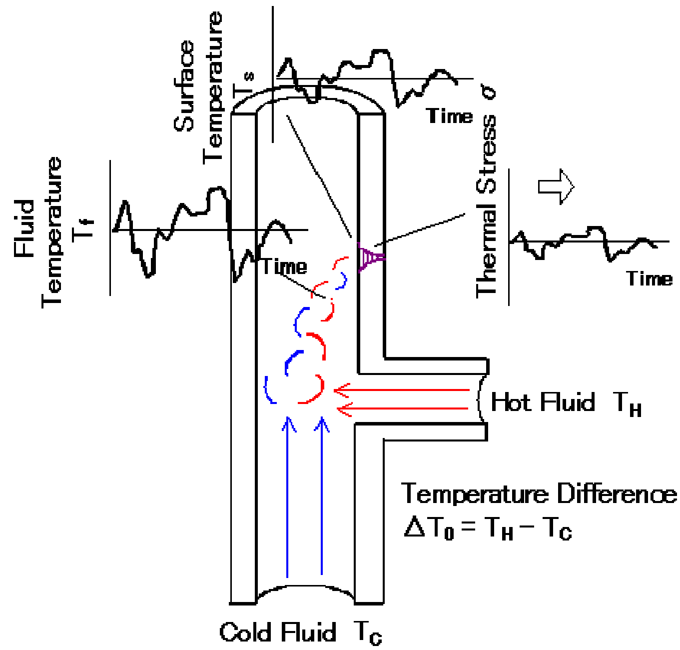

Fig.1 Transfer process from fluid temperature attenuation of structural response

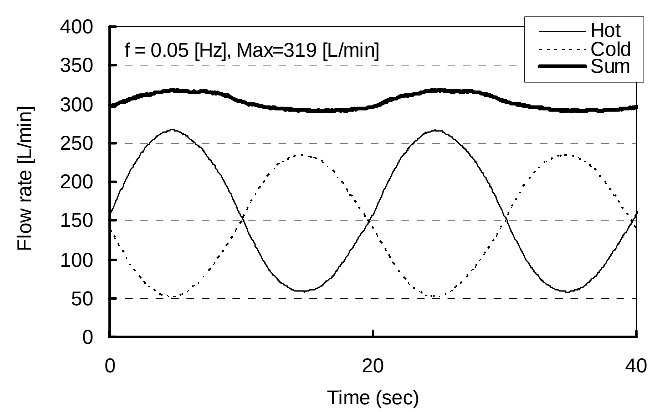

Fig.3 Flow rate of SPECTRA test section

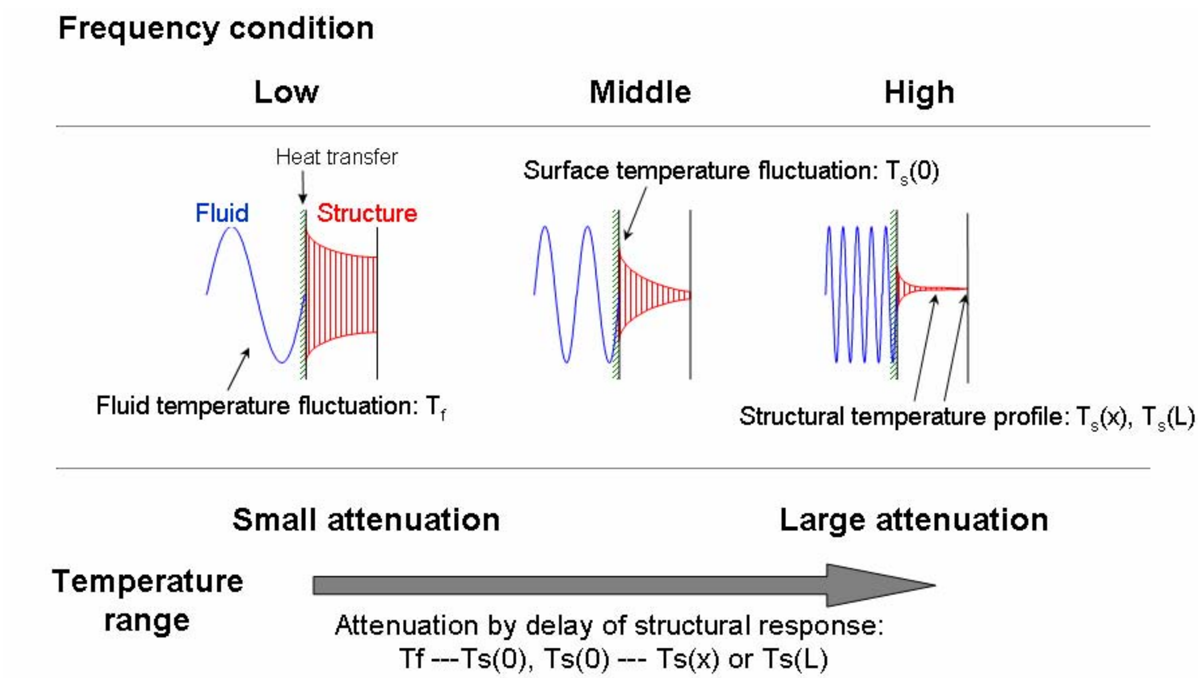

Fig.2 Frequency effect on attenuation of structural response

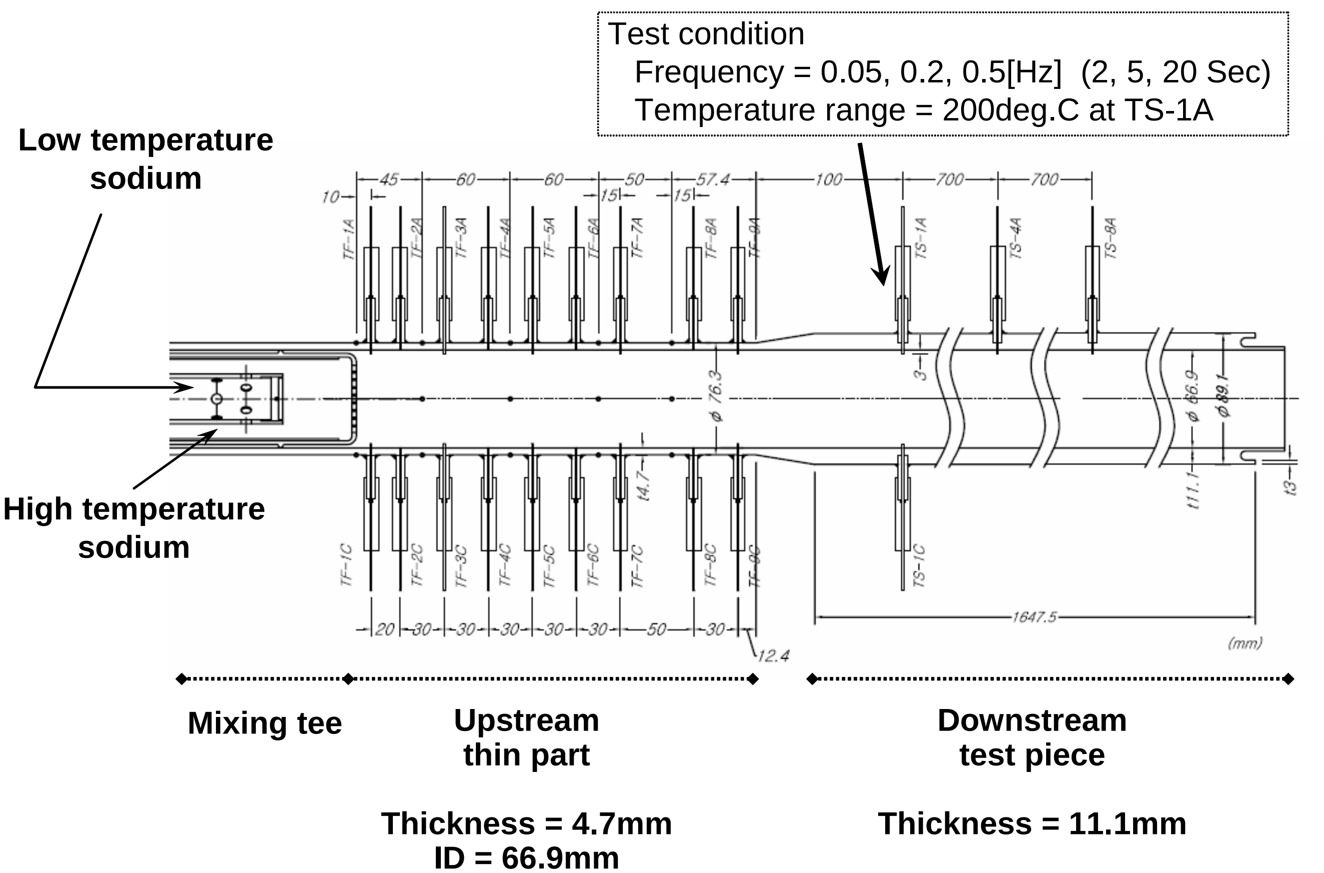

Fig.4 SPECTRA test section

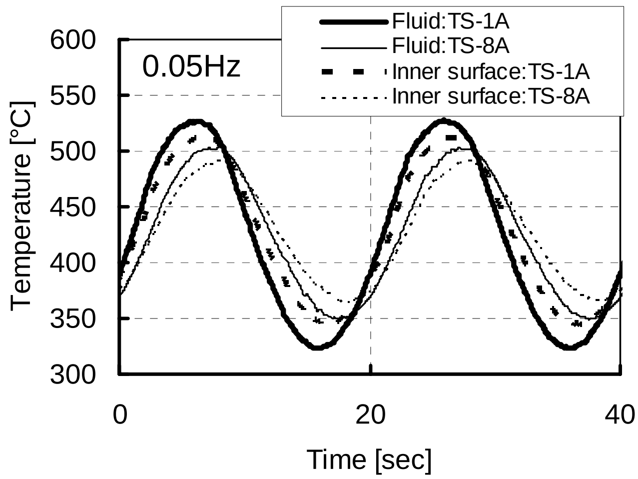

Fig.5 Temperature history: 0.05Hz

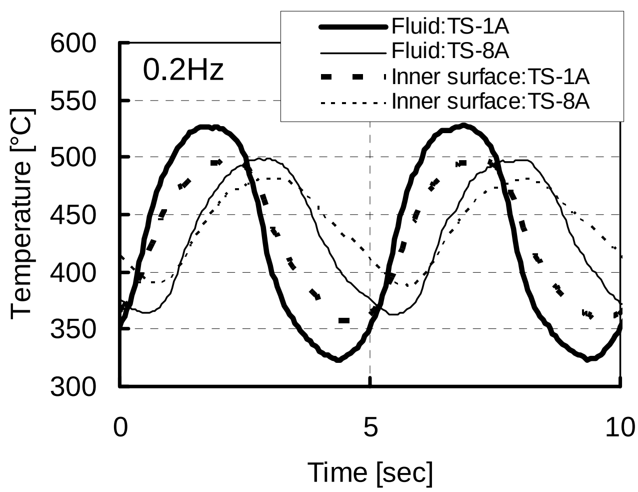

Fig.6 Temperature history: 0.2Hz

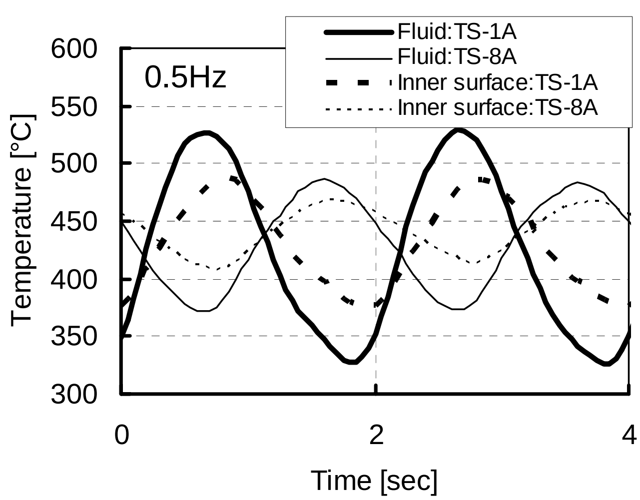

Fig.7 Temperature history: 0.5Hz

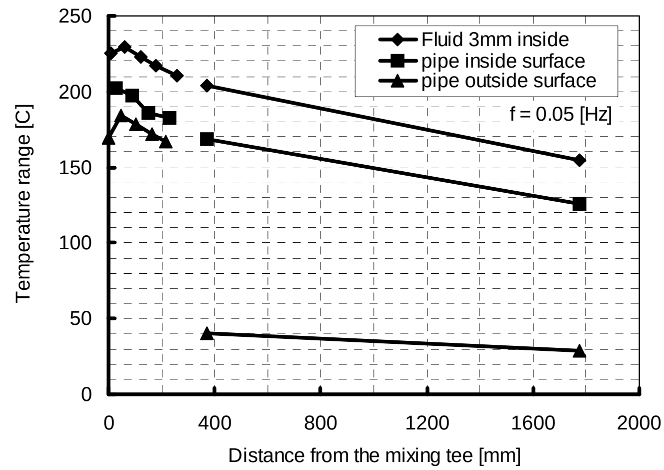

Fig.8 Temperature range of fluctuation: 0.05Hz

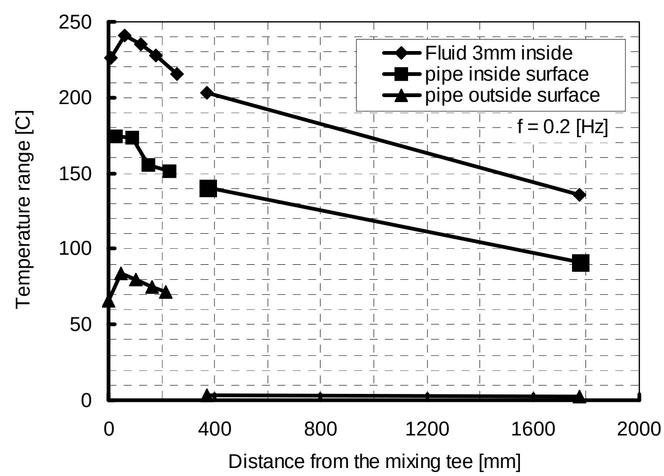

Fig.9 Temperature range of fluctuation: 0.2Hz

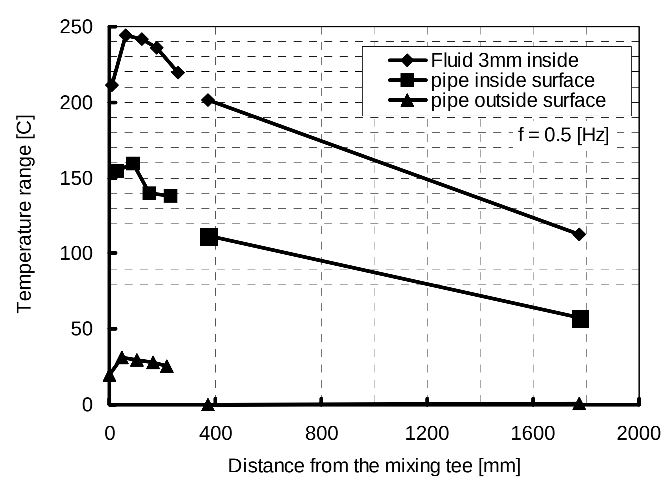

Fig.10 Temperature range of fluctuation: 0.5Hz

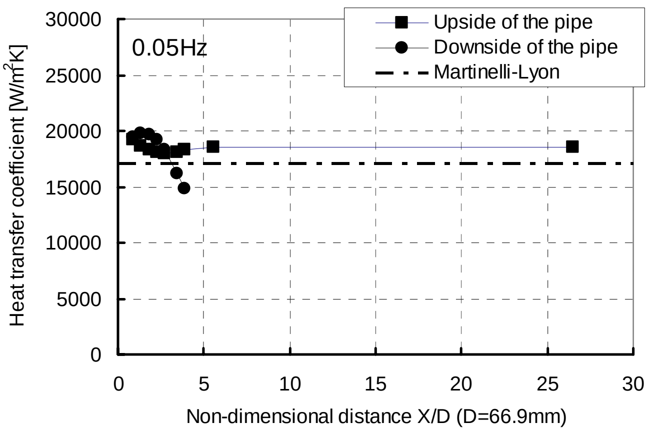

Fig.11 Heat transfer coefficient: 0.05Hz

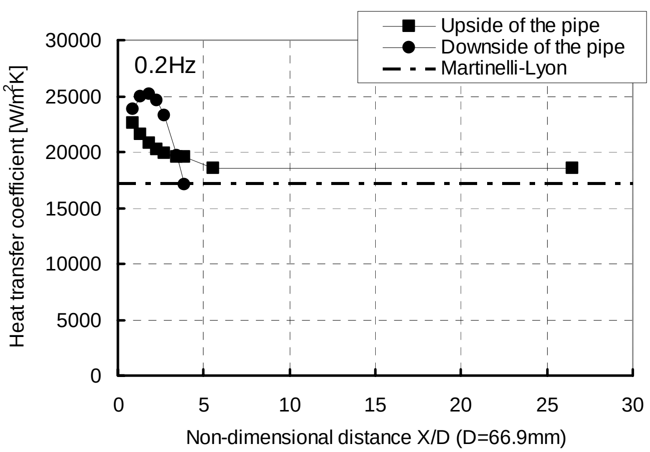

Fig.12 Heat transfer coefficient: 0.2Hz

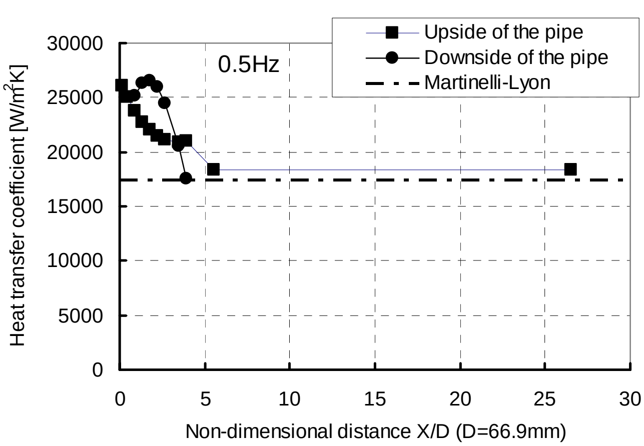

Fig.13 Heat transfer coefficient: 0.5Hz

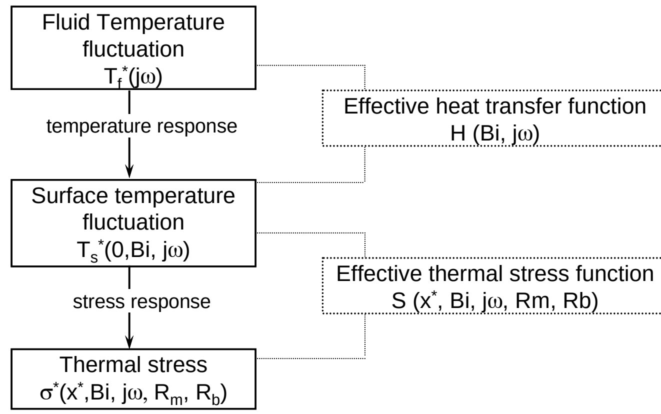

Fig.14 Proposed evaluation procedure with frequency transfer functions

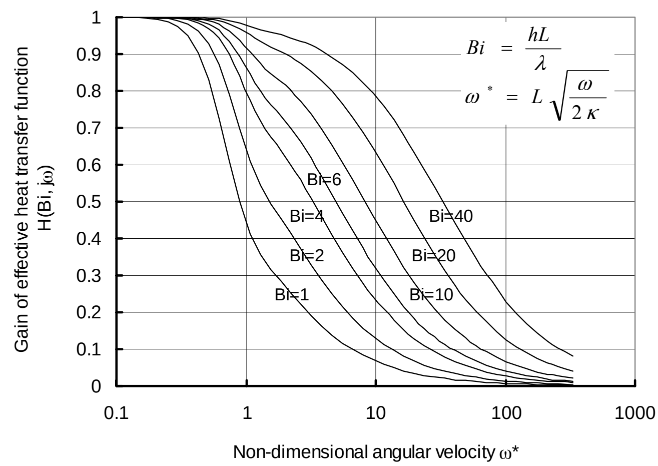

Fig.15 Theoretical effective heat transfer function: H(Bi, jω)

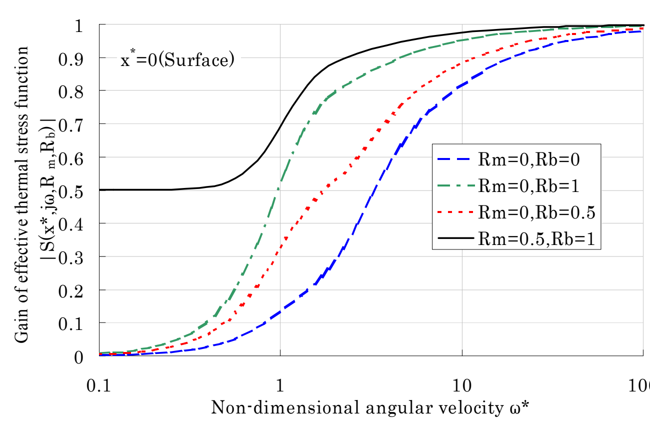

Fig.16 Theoretical effective thermal stress function S(x*, Bi, jω, Rm, Rb): for SPECTRA Rm=0,Rb=1

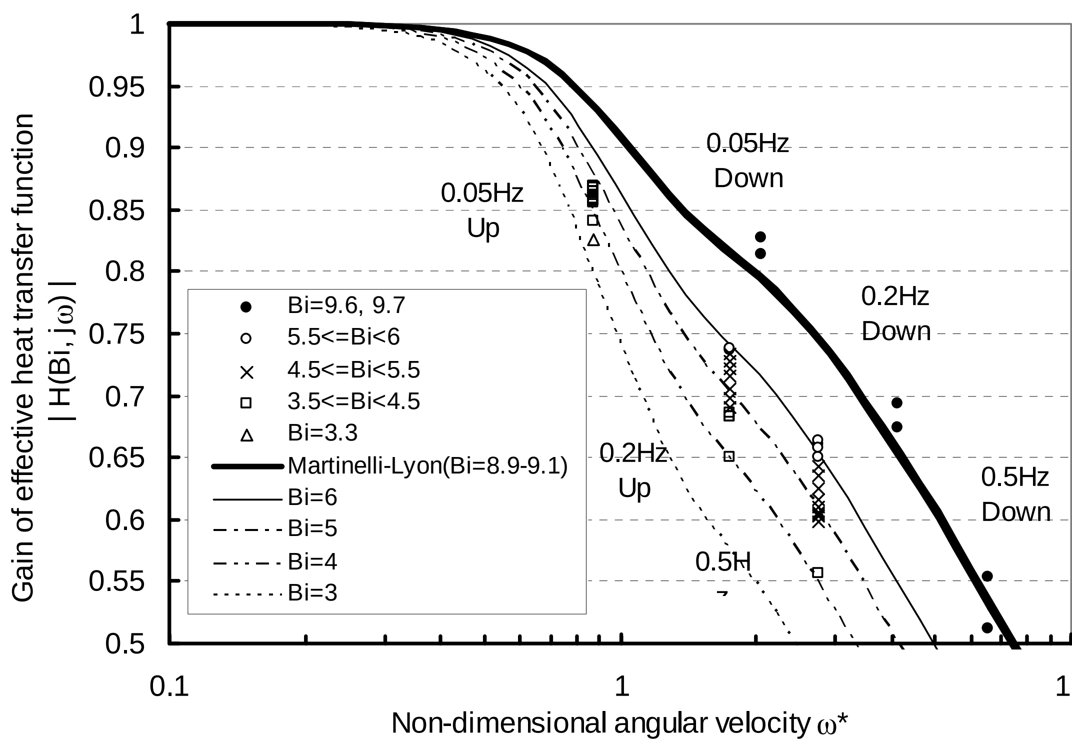

Fig.17 Frequency effect of H(Bi, jω)

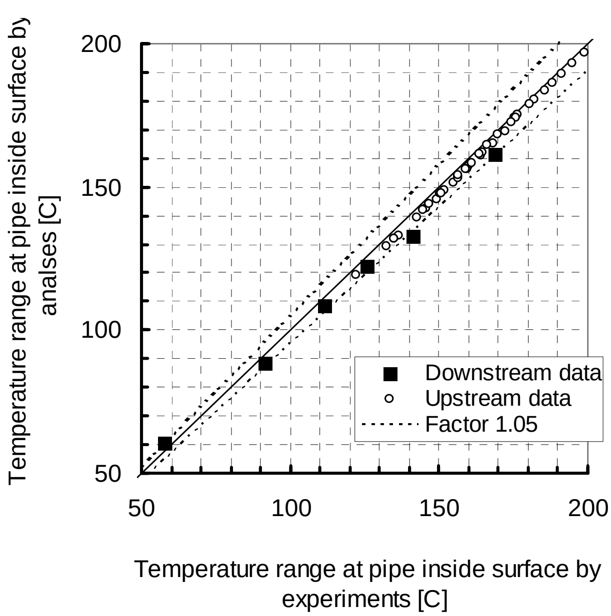

Fig.18 Evaluation accuracy